H-Bonded Complexes of Aniline with HF/F^- and Anilide with HF in Terms of Symmetry-Adapted Perturbation, Atoms in Molecules, and Natural Bond Orbitals Theories

Halina Szatyłowicz*

Faculty of Chemistry, Warsaw University of Technology, Noakowskiego 3, 00-664 Warsaw, Poland

Tadeusz M. Krygowski

Department of Chemistry, Warsaw University, Pasteura 1, 02-093 Warsaw, Poland

Jarosław J. Panek and Aneta Jezierska

National Institute of Chemistry, Hajdrihova 19, 1001 Ljubljana, Slovenia, and Faculty of Chemistry, University of Wrocław, F. Joliot-Curie 14, 50-383 Wrocław, Poland

Received: April 24, 2008; Revised Manuscript Received: July 26, 2008

The hydrogen-bonded isoelectronic complexes of aniline with HF/F^- and an ionic form of aniline with HF were investigated by use of computational methods: Symmetry-Adapted Perturbation Theory (SAPT), Atoms in Molecules (AIM), and Natural Bond Orbitals (NBO) approaches. All computations were based on structural models previously generated at the B3LYP/6-311+(d,p) level. The differences between neutral (Ph−NH_2···HF) and anionic (Ph−NH_2···F^- and Ph−NH^-···HF) complexes were clearly outlined. The discussed charged complexes serve as Lewis acids and base, HF and F^-, respectively. It was found that electrostatic and induction energy terms, obtained as a result of the SAPT method, are most dependent on the type of H-bonding (i.e., charged or neutral). The electrostatic term is the most distinctive between the neutral and charge-assisted hydrogen bonds in the investigated two-body systems, whereas the latter is more significant in the case of weaker interactions (larger H···B distances). Application of Principal Component Analysis (PCA) to energy components obtained from the SAPT procedure indicated that all of them are relatively well intercorrelated. The above-mentioned terms together with the exchange energy terms are the most important contributions of the main principal component, which describes 95% of the total variance. Comparison of AIM parameters in bond critical points for modeled H-bond systems shows a good agreement with those from equilibrium complexes, both experimental and calculated ones. It was found that charged H-bonded complexes exhibit larger fluctuation of electron density and its Laplacian in bond critical points, in line with SAPT analysis. NBO results confirmed the effect of the strength of interaction on property changes both in the region of H-bonding and outside of it. The latter, more distant consequences follow the Bent−Walsh rule for all studied complexes.

I. Introduction

According to well-known definitions,[1] the hydrogen bond is a special type of dipole−dipole interaction; however, it also exhibits some features of covalent bonding.[2−4] Such an interaction exists between an electronegative atom and a hydrogen atom bonded to another electronegative atom. Hydrogen bonds are divided into two main categories, intra- and intermolecular.[5] The presence of such interactions is significant for biologically important systems,[6−8] but not only there; it is also relevant for materials science.[9−11] The role of hydrogen bonding in the biological systems is emphasized, for example, in the nucleic acid base pair structures,[12] secondary elements of protein folds,[13] and stabilization of the biomolecular aggregates.[14] The importance of the intermolecular hydrogen bonds in materials science is highlighted by their role, for example, in the ferroelectric effect and liquid crystals.[15,16] Because hydrogen bonds are almost omnipresent in chemistry, biology, and materials science, another important issue is the investigation of phenomena modifying their properties. In this respect, several concepts are discussed, for example, resonance- and charge-assisted hydrogen bonding.[17−21] Such a classification can be used to rationalize, for example, the enzymatic reaction pathways.[22]

The observable manifestations of hydrogen bonding—such as vibrational and NMR spectral shifts—can be related to the energy of stabilization gained by the formation of the hydrogen-bonded complex. Computational chemistry provides numerous methods[23] to investigate the nature of this interaction, allowing, in many cases, estimation of the H-bond energy or other quantities related to this term. A very interesting tool for studies of H-bonding is the decomposition of energy into particular contributions. However, since the particular terms of the energy decomposition are not quantum observables, they are not uniquely defined, which explains a large number of available partitioning schemes. One of the first successful schemes was that of Kitaura−Morokuma.[24] Other proposals, applicable even for large systems of biochemistry or materials science, were given by Sokalski et al.,[25] Mo et al.,[26−28] Kawamura and Nakai,[29] or Ababou et al.[30] The approach used in the current study, Symmetry-Adapted Perturbation Theory (SAPT),[31] is

* To whom correspondence should be addressed. E-mail: halina@ch.pw.edu.pl. Phone: (+48) 22 234 77 55. Fax: (+48) 22 628 27 41.

10.1021/jp803592v CCC: $40.75
Published on Web 09/09/2008

based on the perturbational calculus applied to the inter- and intramonomer electron excitations. This allows the SAPT energy terms to have a clear physical meaning and provides a route for the development of further, higher-order terms. The interaction energy partitioning techniques are, however, usually global. From the set of theories with the capability of describing local variations of bonding, the Atoms in Molecules (AIM) and Natural Bond Orbitals (NBO) approaches were selected for the current study.

The Atoms in Molecules[32,33] method is considered as one of the most useful methods to investigate diverse interactions since it provides very precise quantitative information on the electronic structure. Starting from the topology of the electron density and its derivative fields, the AIM theory defines in a unique way the concepts of an atom, a chemical bond, and their related properties, for example, atomic charges at atoms or densities in the bond critical points. The AIM-derived descriptors of the molecular structure are less dependent on the theoretical level than the conventional formulations, for example, Mulliken atomic charges. The AIM theory provides numerical means to distinguish between shared electron (covalent) and ionic types of bonds. The borderline case, hydrogen bonding, requires special treatment. A set of criteria to be met by the electronic structure of a hydrogen-bonded system was proposed by Koch and Popelier.[34] These criteria have inspired numerous studies correlating AIM-derived molecular properties with other theoretical and experimental measures of the hydrogen bond strength.[4,35−39] Another well-known application of the AIM theory is the calculation of molecular descriptors for further development of empirical/mathematical models useful to predict quantitative properties, for example, biological activity (QSAR models).[40,41] The AIM methodology has also been successfully applied to systems of biological interest, for example, deoxyribonucleosides[37] and peptides.[42] As an additional tool for electronic structure description, Natural Bond Orbitals (NBO) analysis was carried out to investigate the strength of the intermolecular hydrogen bond of the complexes considered.[43] NBO describes chemical bonding in terms widely used in general chemistry, such as hybridization or charge donation, which facilitates rationalization of the observed changes and trends.

Aniline contains an amine group which can act as both the donor and acceptor of hydrogen bonds. This group lies in close proximity to the aromatic ring, which provides an opportunity to study the influence of substituent effects on the structure and aromaticity indices of the ring and also vice versa, the results of hydrogen bond formation with respect to the properties of the amino group in aniline.[44−47]

The aim of the present study was to investigate the intermolecular H-bonding between aniline and HF or F^- depending on whether the amino group acts as the proton-donating or proton-accepting one. In addition, the anionic form of the aniline derivative and HF interactions was studied. By scanning the proton donor−acceptor separation, a series of structures with different strengths of the hydrogen bond was generated. Understanding the partitioning of the interaction energy of aniline complexes is relevant to one of the basic chemical concepts, the acid−base interaction. A smooth transition between directional, short-range H-bridges, and long-distance weaker forces seems to be significant for such areas as material engineering and explanation of biochemical processes, for example, small-molecule transport or elementary reaction pathways.

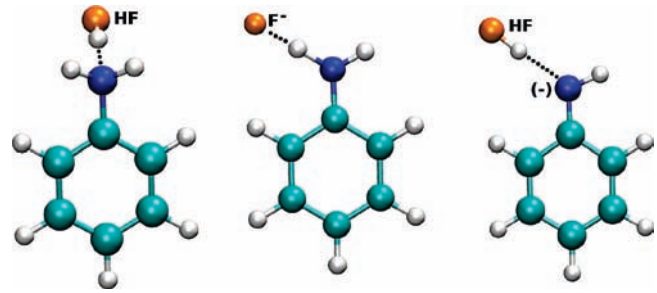

Figure 1. The structures of the investigated aniline complexes: neutral form (left), aniline−F^- anion (middle), and anilide anion−HF (right). The blue color indicates a nitrogen atom. The dotted lines indicate an intermolecular hydrogen bond.

The outline of the article is as follows. The methods applied in the study are presented in section II, the results and discussion are given in section III, whereas the concluding remarks are presented in section IV.

II. Computational Methodology

The geometry of the investigated isoelectronic complexes of aniline with HF and F^- and anilide, the anionic form of aniline, with HF (see Figure 1) was optimized using the density functional theory (DFT) method.[48,49] A three-parameter hybrid functional proposed by Becke[50] with the correlation energy according to the Lee−Yang−Parr formula,[51] denoted as B3LYP, was applied. The triple-ζ split-valence basis set with diffuse functions on non-hydrogen atoms and polarization functions on all atoms (d, non-hydrogen; p, hydrogen), referenced as 6-311+G(d,p),[52] was used. Harmonic frequencies were calculated in order to confirm that the obtained geometry corresponded to minima on the potential energy surface (PES). In the case of the complex of the anionic form of aniline with HF (see Figure 1), the optimization led to the collapse of the structure to the aniline−F^- form.

Starting from the geometries obtained as a result of energy minimization, the potential energy scan was performed by fixing the N···F distances (the linearity of N···H···F was assumed in the scan) and optimizing the remaining internal degrees of freedom in each step of the energy scan using an 0.2 Å increment. For all three studied systems, neutral aniline−HF as well as anionic anilide−HF and aniline−F^- complexes, the values of the distance were scanned from 2.6 to 4.0 Å. In all studied complexes, for the separation of heavy atoms of the H-bond of less than 3.0 Å and for that of aniline−HF equal to 3.0 Å, the structures had only positive frequencies. Only one imaginary frequency was found for the remaining N···F distances, indicating the proper route of the proton on the path realized by H-bonding. During both the geometry optimizations and relaxed PES scans, the wave functions were generated for further application in the Atoms in Molecules (AIM) study. This part of calculations was carried out using the Gaussian03 suite of programs.[53]

The interaction energy decomposition was performed for optimized structures and sets of coordinated data resulting from PES scans on the basis of previously stored electronic integrals and wave functions generated by the GAMESS program.[54] Further computations involved the application of the Symmetry-Adapted Perturbation Theory (SAPT).[31] This technique provides decomposition of the interaction energy and estimation of specific contributions related to the physical concepts such as polarization and dispersion. A particular set of terms calculated in the present study is described by the following equation

$$E^{\mathrm{SAPT}} = E^{10}_{\mathrm{elst}} + E^{10}_{\mathrm{exch}} + E^{20}_{\mathrm{ind,r}} + E^{20}_{\mathrm{exch-ind,r}} + \delta^{\mathrm{HF}}_{\mathrm{int,r}} + E^{12}_{\mathrm{elst,r}} + E^{13}_{\mathrm{elst,r}} + E^{20}_{\mathrm{disp}} + E^{20}_{\mathrm{exch-disp}} + {}^{\mathrm{t}}E^{22}_{\mathrm{ind}} + {}^{\mathrm{t}}E^{22}_{\mathrm{exch-ind}} + \varepsilon^{1}_{\mathrm{exch}}(\mathrm{CCSD}) + \varepsilon^{2}_{\mathrm{disp}}(2) \quad (2)$$

The basic contributions to the interaction energy are E^{10}_{elst} (electrostatic interaction of frozen charge distributions of the monomers), E^{10}_{exch} (repulsion force due to the quantum exchange phenomenon), $E^{20}_{\mathrm{ind,r}}$ (the result of mutual polarization of charge distributions of the monomers), and $E^{20}_{\mathrm{exch-ind,r}}$ (correction to the exchange resulting from polarization). These terms do not include intramonomeric electron correlation. Together with a correction term δHF, they correspond to the Hartree−Fock interaction energy. From the set of correlation corrections, we report the most important ones, E^{20}_{disp} (dispersion energy) and $E^{20}_{\mathrm{exch-disp}}$ (contributions to exchange repulsion resulting from dispersion effects). ${}^{\mathrm{t}}E^{22}_{\mathrm{ind}}$ and ${}^{\mathrm{t}}E^{22}_{\mathrm{exch-ind}}$ provide additional contributions to the induction and exchange terms, making the resulting interaction energy comparable to the second-order MP2 value. The addition of the $\varepsilon^{1}_{\mathrm{exch}}$(CCSD) and $\varepsilon^{2}_{\mathrm{disp}}(2)$ terms (respectively, the exchange contribution calculated with intramonomer excitations at the CCSD level and an additional dispersion term to complete the second-order intramolecular expansion) raises the accuracy of the SAPT energy to approximately a fourth-order perturbational level.

The SAPT method is traditionally associated with rather weak intermolecular forces in dimeric systems, such as in Ar−H_2 and $(CO_2)_2$ complexes.[55] However, it has found applications in the analysis of the interaction energy of hydrogen-bonded many-body systems as well as for stacking structures as reported in literature.[56] The SAPT analysis in the current study was performed using the SAPT2006 program.[57]

Atoms in Molecules (AIM)[32] theory was applied to investigate the topology of electron density and intermolecular hydrogen bond properties of the studied structures. The chemical bonding topology was investigated by confirming the presence of relevant bond paths and analysis of bond critical points, with special attention paid to the intermolecular H-bonding. The properties of the intermolecular H-bond were investigated by application of Popelier's criteria.[58] The AIM analysis was carried out using the AIMPAC package.[59]

Natural Bond Orbitals (NBO)[43] analysis (Gaussian NBO,[60] version 3.1) was used to study the effect of H-bonding strength on the occupancy at the "lone pair" orbital of the nitrogen atom (LP) and at CN bonds (σ- and π-bond) and hybridization changes at the carbon atom (substituted by NH_2 or NH^-) reflected in electronic properties of the CN bond and *ortho*−*ipso*-CC bonds of the benzene ring. The former explains the properties alteration at the atom participating in H-bonding, whereas the latter allows one to observe short-distance consequences of the interaction.

The graphical presentation of the studied complexes was prepared using the VMD program.[61]

III. Results and Discussion

The purpose of this work was to investigate H-bonding interactions analyzed by employing three different strategies, (i) the energy decomposition applying Symmetry-Adapted Perturbation Theory, SAPT,[31] (ii) electron density topology applying Atoms in Molecules theory, AIM,[32−34] and (iii) using Natural Bond Orbitals, NBO model.[43] All of them were applied to three H-bonded complexes of aniline derivatives presented in Figure 1.

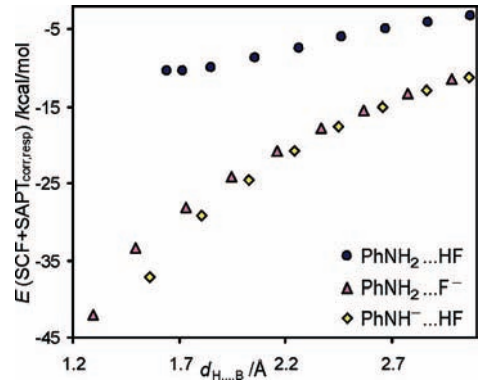

Figure 2. Estimated interaction energy as a function of hydrogen bond length, $d_{\mathrm{H}\cdots\mathrm{B}}$, in complexes of aniline with HF and F$^-$ and the ionic form of aniline with HF.

An important feature of the present study is the fact that the changes in H-bond strength are realized with a Lewis acid and base pair, HF and F$^-$, respectively, interacting with aniline or the anilide anion. Thus, the results and conclusions are not biased by various structural changes of acid and bases interacting with aniline or anilide, which occur in the case where the experimental interacting systems are investigated. For clarity, these three approaches are presented separately, with a joint conclusion presented at the end of the paper.

Application of SAPT. The effect of the hydrogen bond length on the strength of interaction, for all of the discussed systems, is presented in Figure 2. It results from the scatter plots and data of Tables 1−3 that the ionic H-bonds $PhNH_2\cdots F^-$ and $PhNH^-\cdots HF$ are much stronger than the nonionic $PhNH_2\cdots HF$. Moreover, for the two ionic H-bonded systems for the shortest H···F distance, both systems achieve a joint point at which this distance is exactly the same. It is worth mentioning that E(SCF+ SAPT$_{corr,resp}$) values are almost identical to the interaction energies computed as a difference between the energy of the H-bonded complex and their participants (monomers), but only for internal coordinates like those in the complex (including Basis Set Superposition Error (BSSE)[62]). It should be stressed here that although the H···B interatomic distance is well accepted as a numerical measure of H-bond strength and the monotonic relations between the energy and H···B distance support this kind of reasoning, the quantitative dependences are different for different kinds of complexes. Similar relationships were found for the $H_2O\cdots HOH$ and $[HOH\cdots OH]^-$ systems,[63] where varying strength of interaction was simulated by the changes of O···O separation.

Basic components of the interaction energy calculated on the basis of the Symmetry-Adapted Perturbation Theory (SAPT) method[31] are shown in Figure 3 as a function of the H-bond length, $d_{\mathrm{H}\cdots\mathrm{B}}$. It should be noted that also in these cases, the presented contributions to the total energy of interactions for charged complexes are usually greater (as absolute values) than those for the neutral ones. Moreover, the range of variability is similar to the changes of electrostatic energies. Interestingly, the E^{10}_{exch} terms form only one curve (Figure 3b), independent of whether the points are for ionic or nonionic species; almost alike, but not exactly, are the points for $E^{20}_{\mathrm{exch,ind}}$ (Figure 3d), whereas this is not the case for the other two components (Figure 3a and c). This is due to an obvious fact that E^{10}_{elst} and $E^{20}_{\mathrm{ind,r}}$ depend on charge interactions in the system.

We will start our discussion from the neutral aniline−HF complex. In this case, the lone electron pair of the aniline nitrogen atom acted as an acceptor in the hydrogen bridge (see Figure 1).

TABLE 1: The Partitioning of the Interaction Energy Obtained for the Neutral Aniline and HF Complex Using Symmetry-Adapted Perturbation Theory[a]

N···F distance /Å	2.6	2.670[b]	2.8	3.0	3.2	3.4	3.6	3.8	4.0
N···H distance /Å	1.640	1.715	1.850	2.057	2.263	2.467	2.670	2.872	3.073
E_{int}^{HF}	−8.87	−9.11	−9.01	−8.12	−6.92	−5.73	−4.66	−3.79	−3.11
E_{elst}^{10}	−21.55	−18.88	−14.95	−10.71	−7.91	−5.99	−4.62	−3.64	−2.95
E_{exch}^{10}	24.81	19.49	12.51	6.30	3.16	1.59	0.79	0.40	0.20
$E_{ind,resp}^{20}$	−16.28	−12.97	−8.63	−4.75	−2.70	−1.59	−0.96	−0.60	−0.39
$E_{ex-ind,r}^{20}$	9.02	7.10	4.56	2.32	1.18	0.60	0.31	0.16	0.08
SAPT SCF_{resp}	−4.01	−5.26	−6.51	−6.84	−6.26	−5.39	−4.48	−3.69	−3.06
$\delta_{int,r}^{HF}$	−4.86	−3.86	−2.50	−1.28	−0.66	−0.34	−0.18	−0.10	−0.05
$\varepsilon_{exch}^{(1)}$(CCSD)	3.36	2.84	2.07	1.25	0.74	0.43	0.25	0.14	0.08
$E_{disp}^{2}(k)$	−5.66	−4.79	−3.55	−2.26	−1.48	−0.99	−0.68	−0.47	−0.34
$E_{exch-disp}^{20}$	1.13	0.91	0.61	0.32	0.17	0.09	0.04	0.02	0.01
$SAPT_{corr,resp}$	−1.61	−1.30	−0.94	−0.64	−0.48	−0.37	−0.29	−0.22	−0.17
$SCF+SAPT_{corr,resp}$	−10.47	−10.41	−9.96	−8.76	−7.40	−6.10	−4.95	−4.01	−3.28

[a] The chosen SAPT contributions are given in kcal/mol. [b] The distance was obtained as a geometry minimization result.

TABLE 2: the Partitioning of the Interaction Energy Obtained for the Neutral Aniline and the F^- Anion Complex Using Symmetry-Adapted Perturbation Theory[a]

N···F distance /Å	2.450[b]	2.6	2.8	3.0	3.2	3.4	3.6	3.8	4.0
H···F distance /Å	1.296	1.499	1.731	1.947	2.158	2.366	2.570	2.775	2.978
E_{int}^{HF}	−39.03	−31.94	−27.12	−23.45	−20.22	−17.39	−14.98	−12.95	−11.28
E_{elst}^{10}	−55.71	−39.02	−27.13	−20.34	−16.01	−13.05	−10.92	−9.33	−8.09
E_{exch}^{10}	62.41	33.96	16.58	8.44	4.40	2.34	1.26	0.69	0.39
$E_{ind,resp}^{20}$	−46.09	−28.07	−17.78	−12.52	−9.33	−7.20	−5.67	−4.56	−3.74
$E_{ex-ind,r}^{20}$	18.67	10.13	5.11	2.75	1.55	0.89	0.52	0.30	0.18
SAPT SCF_{resp}	−20.73	−23.01	−23.22	−21.66	−19.40	−17.02	−14.82	−12.89	−11.27
$\delta_{int,r}^{HF}$	−18.31	−8.94	−3.90	−1.78	−0.82	−0.37	−0.16	−0.06	−0.01
$\varepsilon_{exch}^{(1)}$(CCSD)	10.69	7.69	5.11	3.38	2.22	1.44	0.93	0.60	0.39
$E_{disp}^{2}(k)$	−12.03	−7.87	−4.88	−3.17	−2.12	−1.44	−1.00	−0.70	−0.50
$E_{exch-disp}^{20}$	3.64	2.27	1.27	0.73	0.42	0.25	0.14	0.09	0.05
$SAPT_{corr,resp}$	−2.92	−1.57	−0.95	−0.72	−0.60	−0.51	−0.43	−0.35	−0.29
$SCF+SAPT_{corr,resp}$	−41.96	−33.51	−28.08	−24.16	−20.81	−17.90	−15.41	−13.30	−11.56

[a] The chosen SAPT contributions are given in kcal/mol. [b] The distance was obtained as a geometry minimization result.

TABLE 3: The Partitioning of the Interaction Energy Obtained for the Aniline Anion and HF Complex Using Symmetry-Adapted Perturbation Theory[a]

N···F distance /Å	2.6	2.8	3.0	3.2	3.4	3.6	3.8	4.0
N···H distance /Å	1.560	1.805	2.027	2.240	2.449	2.656	2.860	3.064
E_{int}^{HF}	−37.87	−30.09	−25.20	−21.32	−18.15	−15.54	−13.40	−11.65
E_{elst}^{10}	−45.76	−33.55	−26.15	−21.11	−17.47	−14.75	−12.64	−10.99
E_{exch}^{10}	32.71	15.95	8.20	4.31	2.29	1.23	0.67	0.37
$E_{ind,resp}^{20}$	−25.83	−14.25	−8.59	−5.40	−3.50	−2.33	−1.60	−1.13
$E_{ex-ind,r}^{20}$	11.12	6.33	3.64	2.09	1.19	0.68	0.39	0.22
SAPT SCF_{resp}	−27.76	−25.52	−22.90	−20.11	−17.48	−15.17	−13.18	−11.53
$\delta_{int,r}^{HF}$	−10.11	−4.57	−2.31	−1.22	−0.66	−0.37	−0.21	−0.13
$\varepsilon_{exch}^{(1)}$(CCSD)	6.16	3.64	2.28	1.44	0.91	0.57	0.36	0.23
$E_{disp}^{2}(k)$	−7.67	−4.49	−2.83	−1.85	−1.24	−0.85	−0.59	−0.42
$E_{exch-disp}^{20}$	1.71	0.92	0.50	0.27	0.15	0.08	0.05	0.03
$SAPT_{corr,resp}$	0.57	0.79	0.74	0.63	0.54	0.48	0.43	0.40
$SCF+SAPT_{corr,resp}$	−37.29	−29.30	−24.47	−20.69	−17.60	−15.06	−12.96	−11.25

[a] The chosen SAPT contributions are given in kcal/mol.

The results obtained for the discussed complex are presented in Table 1. In the position of the potential energy minimum, we observe an almost perfect mutual canceling out between the first-order contributions, the electrostatic and exchange energies. It is worth emphasizing that in the case of neutral partners, both mentioned energies are the most important contributions, in agreement with the findings for diverse H-bonded complexes of phenol and water with various neutral molecules.[64] It is also important to note that this canceling out of those two terms does not work for nonequilibrium states with longer or shorter N···F distances than that in equilibrium state. The exchange energy term, which arises from the short-range Pauli's repulsion is most sensitive to variations of the H...B interatomic distance. The neglect of intramonomer electron correlation would lead to the optimal N···F distance between monomers enlarged to ∼3.0 Å, the minimal value of the SAPT SCF_{resp} term. A detailed analysis of the interaction energy allowed us to classify the studied complex as belonging to the class of middle strong hydrogen bonds.[3,5] A comparison of the total correlated contribution ($SAPT_{corr,resp}$) and final interaction energy ($SCF+SAPT_{corr,resp}$) indicates that dispersion terms are not crucial for the proper description of this type of interaction. At this point, we would like to point out that the SAPT results for the neutral aniline−HF complex, described in detail above, are in agreement with our earlier investigations. Such a type of

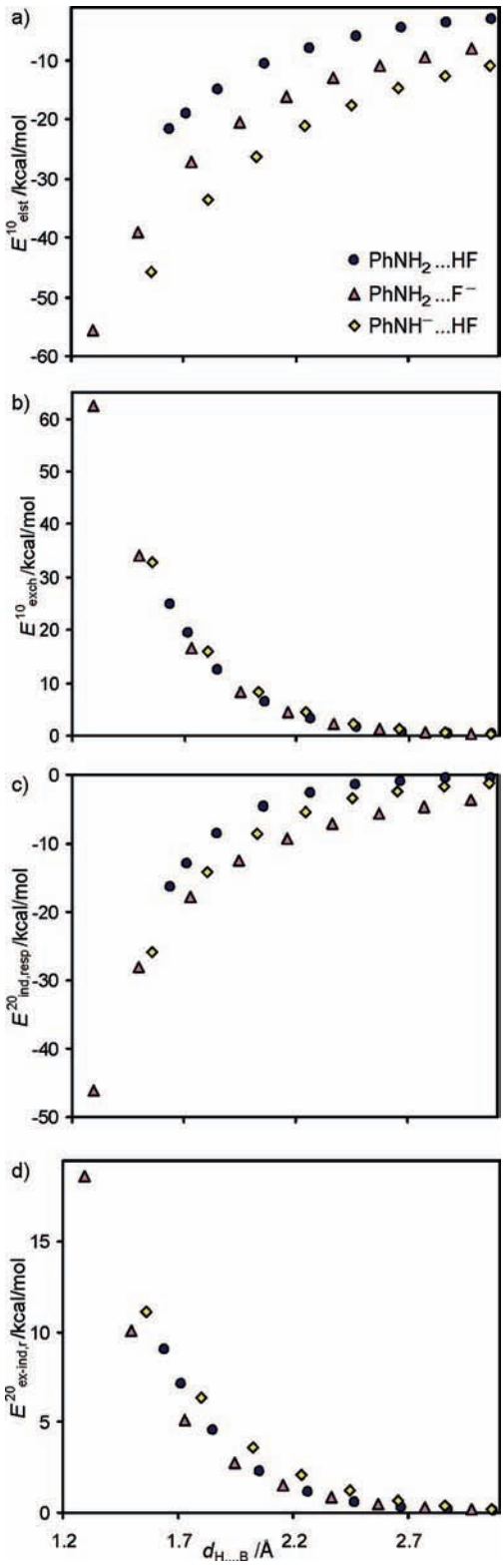

Figure 3. Relationship between basic contributions to the interaction energy and H-bond length, $d_{H\cdots B}$, for complexes of aniline with HF and F^- and the anilide anion with HF.

analysis was successfully applied for the directionality and angular dependence of N···HX complexes.[65]

Tables 2 and 3 report the results for ionic forms of the studied complexes. In Table 2, the charged moiety is F^-, whereas the neutral one is aniline. In Table 3, the charged species is the anilide anion, which interacts with HF. Such complexes represent examples of charge-assisted hydrogen bonds.[18] As a result, the most striking difference between the neutral and charged forms of the H-bonded systems is a significantly higher value of the total interaction energy, in terms of absolute values (three to four times higher as compared with the above-discussed neutral complex). This effect is pronounced already at the SCF level (see the SAPT SCF_{resp} energy), and the correlated terms do not contribute significantly to the total interaction energy. Interestingly, the sum of correlated contributions provides additional stabilization for the aniline···F^- complex, but it destabilizes the anilide···HF system. In contrast to the neutral form (see Table 1), the electrostatic term, E^{10}_{elst}, is dominating over the exchange energy, E^{10}_{exch}, in the investigated range of distances. The exchange contribution describes the effects of overlap of orbitals, and it is roughly similar in the charged and neutral cases, being larger for the anionic systems because of a more diffuse electron density of anionic species. The reason for strengthening of the H-bond in anionic species, the source of the charge-assisted effect, is provided by the E^{10}_{elst} contribution. It describes the interaction of frozen multipoles, and it is necessarily larger and covers longer distances when one of the monomers is charged. A similar effect is also visible for the induction term $E^{20}_{ind,resp}$, which suggests that the anions are more polarizable than their corresponding neutral analogues. By comparing the two anionic species, one can notice that the total interaction energies are rather similar, especially for long distances, where the approximation of ion−dipole interaction is more important. The dispersion contribution $E^{2}_{disp}(k)$ is slightly larger when the anion is F^-. As a final remark to the SAPT study, we would like to point out that the $\delta^{HF}_{int,r}$ term starts to be significant at N···F distances lower than 3.2 Å. The covalent nature of the hydrogen bond is partially revealed in this contribution, which contains "higher-order" corrections not explained at the applied SAPT level. Additionally, the studied systems exhibit a regular dependence of exchange energy on the N···F distance; the E^{10}_{exch} term is halved when the distance increases by 0.2 Å. These findings are in agreement with previous observations for ammonia−HF complexes.[65]

When the independent data from Tables 1−3 are processed by the principal component analysis,[66] a very important result appears; the main principal component, PC1, describes >95.2% of the total variance. The second principal component, PC2, accounts for only 4.3%, all other being meaningless (less than 0.5%). Deeper analysis of the components in PC1 shows that the most important contributions are E^{10}_{elst}, E^{10}_{exch}, and $E^{20}_{ind,resp}$. Moreover, in the PC2, the first two contributions mentioned above are also the most important. Such a high percentage of the total variance explained by the PC1 means that most of the contributions of the decomposed energy are mutually correlated. This is most probably due to the fact that in all three series of the considered systems, the structural changes of basic/acidic partners of aniline and anilide are very small, between either F^- or HF.

Application of AIM. The second part of the computational study was devoted to topological investigations into the electron density distribution in the examined complexes. The Atoms in Molecules (AIM) theory gave insight into electron density fluctuations resulting from the formation and modification of the hydrogen bridge. Even if rigorous formulation of the AIM theory requires that all calculations be carried out at the equilibrium geometry, the method was found to be a valuable source of information on the structure-induced modifications of properties of hydrogen bonds.[2,67] Following these nonequilibrium structure studies, we will use below the AIM terminology (especially the bond critical point) for both the equilibrium

CHART 1: The Neutral Complex Aniline···HF[a]

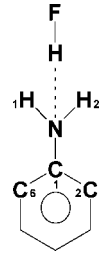

[a] Atoms significant for the discussion are labeled.

CHART 2: The Aniline···F⁻ Complex[a]

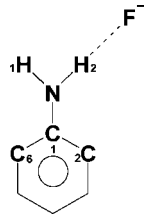

[a] Atoms significant for the discussion are labeled.

CHART 3: The Anilide···HF Complex[a]

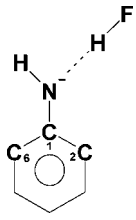

[a] Atoms significant for the discussion are labeled.

and modified geometries since our purpose is not to prove or disprove existence of a hydrogen bond in a doubtful case but to carry out analysis of the variability of electronic density in the neighborhood of a strong N···F hydrogen bond. Simulated systems with gradual variation of the strength of the H-bond enable us to study the effect of intermolecular interaction on electronic and structural changes without additional disturbances, for example, intramolecular interactions such as substituent effects.[47]

Application of AIM to all three kinds of the discussed complexes allowed us to find bond critical points, BCP, and analyze their properties (electron density, ρ, its Laplacian, $\nabla^2\rho$, the electron energy density, H_{CP}, and the kinetic, G_{CP}, and potential, V_{CP}, electron energy density). The atoms relevant for the AIM analysis are shown in Charts 1−3.

The analysis of the electron density topology is presented in Figure 4. The cross sections indicate deep mutual penetration of electron densities of the monomers, which is expected for the investigated strong interactions. The presence of atomic interaction paths with respective critical points, the first criterion,[34,58] was confirmed for all three systems in the whole investigated range of distances. The Popelier's criteria[34,58] were applied to the critical point describing H-bond formation (N···H for the aniline−HF and anilide anion−HF complexes; H2···F for the aniline−F^- complex). These criteria require that the critical points fulfill the following conditions: the electron density at the bond critical point (BCP) at the hydrogen bridge is in the range of 0.002−0.034 au (second Popelier's criterion) while its Laplacian is between 0.024 and 0.139 au (third Popelier's criterion). Formally, these conditions should be met at the equilibrium geometry. The lower limit of the second criterion is fulfilled by all of the studied complexes, but the third one is fulfilled only by the systems with the separation between heavy atoms of the H-bond equal to or shorter than 3.4 Å; see Tables 4−6 and Figure 5. Since our data model the H-bond for different, usually nonequilibrium, intermolecular H···B distances, in Figure 5, we compare these results with those obtained for equilibrium states[4] (MP2/6-311++G(d,p) data). As we can see, there is a very good qualitative agreement between these two sets of presented data. This agreement supports our choice of systems and methodology for H-bond modeling.

As it is well-known,[2,4,68] the total electron energy density, H_{CP}, at the BCP characterizes the nature and the strength of the interaction. Its negative value suggests a partly covalent character of the H-bond. In the case of strong hydrogen bond, the Laplacian is also negative; this indicates the shared interaction, that is, the covalent bond.[2,4] Figure 6 shows a relationship between the total electron energy density, H_{CP}, its components (the kinetic, G_{CP}, and potential, V_{CP}, parts), and the H-bond proton-acceptor distance. Only two of our systems are fully optimized; therefore, for comparison, a set of 25 H-bonded complexes investigated by Grabowski et al.[4] was added in Figure 6. Again, the obtained relationships are very similar and, which is even more important, agree with the experimental data.[38,39] These good agreements (Figures 5 and 6) convince us that nonequilibrium H-bonded complexes with gradual changes in the strength of interaction are reliable systems for the presented consideration.

Let us start our discussion of the electron density (ρ) and its Laplacian ($\nabla^2\rho$) fluctuations in the investigated complexes with the description of the neutral system (Chart 1). In this case, the previous SAPT analysis (see the text above) indicates the presence of the middle strong hydrogen bond. Table 4 collects the values of ρ and $\nabla^2\rho$ as a function of the N···F distance for neutral aniline···HF complexes. All of the changes are rather small. Both the ρ and $\nabla^2\rho$ values in the BCP of the C−N bond become larger (as absolute values) when the N···F distance is lengthened. These parameters are almost constant for the BCP of both N−H bonds. A greater change is observed for N···HF interactions. As expected, an increase of the N···F distance leads to a lowering of the H-bond strength, and hence, ρ and $\nabla^2\rho$ values decrease for the BCP of the N···H bond and increase (in absolute value) for the H−F bond.

A different situation is found for ionic interactions, as can be seen from the data in Tables 5 and 6. In the case of the aniline···F^- complex (Chart 2), the electron densities in the BCPs of N−H in the N−H1 and N−H2 bonds differ dramatically. The one involved in H-bonding (N−H2) has the lowest value of ρ in the optimal complex (0.2172 e·a_0^{-3}), and an increase of the N···F distance leads to an increase of ρ. For the N···F separation equal to 4.0 Å, the electron density approaches the value for another bond, N−H1, which is not involved in the H-bonding. Note that H-bond formation, N−H2···F^-, practically does not affect the electron density value in the BCP for N−H1. It is important to emphasize that both the ρ and $\nabla^2\rho$ values in the BCP of the CN bond decrease (as absolute values) with an increase of the N···F intermolecular distance. Thus, the strength of the CN bond increases (its shortening is observed) with an increase of the H-bonding strength, which may be expressed by an increase of ρ and total electron density (as absolute values, Figure 6) values in the BCP of the the H-bond (H2···F). A reverse trend is observed for the N−H2 bond.

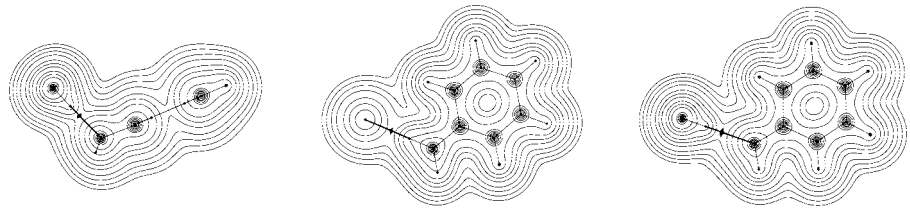

Figure 4. The cross sections of electron density including AIM interatomic paths of complexes of aniline with HF (left) and F$^-$ (middle) and the ionic form of aniline with HF (right). The paths of the intermolecular hydrogen bonds are marked by thick lines, and the corresponding hydrogen bond critical points are located by rhomb marks. The cross section on the left is perpendicular to the aromatic ring plane along the CN bond and includes the intermolecular H-bond, whereas the remaining graphs are plotted in the plane of the phenyl ring.

TABLE 4: The AIM Analysis Results for the Neutral Aniline−HF Complex (electron densities in e·a$_0^{-3}$; electron density Laplacians in e·a$_0^{-5}$) at Selected Critical Points (see Chart 1)

	C−N		N−H1		N−H2		N···H		H−F	
N···F distance /Å	ρ	$\nabla^2\rho$	ρ	$\nabla^2\rho$	ρ	$\nabla^2\rho$	ρ	$\nabla^2\rho$	ρ	$\nabla^2\rho$
2.6	0.2785	−0.7870	0.3369	−1.5534	0.3370	−1.5545	0.0603	0.1142	0.3199	−2.2006
2.670[a]	0.2796	−0.7923	0.3371	−1.5540	0.3371	−1.5536	0.0504	0.1075	0.3244	−2.2780
2.8	0.2813	−0.8001	0.3374	−1.5546	0.3374	−1.5547	0.0364	0.0915	0.3319	−2.3946
3.0	0.2836	−0.8107	0.3378	−1.5562	0.3378	−1.5562	0.0227	0.0641	0.3413	−2.5206
3.2	0.2855	−0.8193	0.3381	−1.5578	0.3381	−1.5577	0.0146	0.0412	0.3484	−2.6053
3.4	0.2872	−0.8264	0.3384	−1.5586	0.3384	−1.5590	0.0095	0.0257	0.3538	−2.6639
3.6	0.2887	−0.8327	0.3387	−1.5612	0.3386	−1.5606	0.0063	0.0161	0.3578	−2.7040
3.8	0.2899	−0.8375	0.3389	−1.5619	0.3388	−1.5613	0.0042	0.0104	0.3607	−2.7318
4.0	0.2905	−0.8405	0.3389	−1.5598	0.3388	−1.5597	0.0027	0.0069	0.3627	−2.7498

[a] N···F distance of the optimal B3LYP/6-311+G(d,p) structure.

TABLE 5: The AIM Analysis Results for the Aniline−F$^-$ Complex (electron densities in e·a$_0^{-3}$; electron density Laplacians in e·a$_0^{-5}$) at Selected Critical Points (see Chart 2)

	C−N		N−H1		N−H2		H2···F	
N···F distance /Å	ρ	$\nabla^2\rho$	ρ	$\nabla^2\rho$	ρ	$\nabla^2\rho$	ρ	$\nabla^2\rho$
2.450[a]	0.3301	−0.9927	0.3377	−1.4595	0.2172	−0.7620	0.1178	0.1510
2.6	0.3250	−0.9770	0.3391	−1.4985	0.2566	−1.1738	0.0692	0.1642
2.8	0.3197	−0.9628	0.3397	−1.5207	0.2840	−1.4033	0.0392	0.1109
3.0	0.3158	−0.9510	0.3399	−1.5318	0.2995	−1.5035	0.0242	0.0697
3.2	0.3129	−0.9407	0.3400	−1.5392	0.3098	−1.5584	0.0156	0.0439
3.4	0.3108	−0.9322	0.3400	−1.5444	0.3169	−1.5894	0.0102	0.0286
3.6	0.3092	−0.9252	0.3400	−1.5480	0.3219	−1.6064	0.0068	0.0190
3.8	0.3079	−0.9193	0.3400	−1.5512	0.3256	−1.6161	0.0045	0.0126
4.0	0.3067	−0.9137	0.3400	−1.5547	0.3286	−1.6227	0.0030	0.0085

[a] N···F distance of the optimal B3LYP/6-311+G(d,p) structure.

TABLE 6: The AIM Analysis Results for the Aniline Anion−HF Complex (electron densities in e·a$_0^{-3}$; electron density Laplacians in e·a$_0^{-5}$) at Selected Critical Points (see Chart 3)

	C−N		N−H		N···H		H−F	
N···F distance /Å	ρ	$\nabla^2\rho$	ρ	$\nabla^2\rho$	ρ	$\nabla^2\rho$	ρ	$\nabla^2\rho$
2.6	0.3381	−1.0268	0.3329	−1.3620	0.0756	0.0648	0.2432	−1.3705
2.8	0.3400	−1.0343	0.3319	−1.3425	0.0419	0.0756	0.2815	−1.8910
3.0	0.3413	−1.0390	0.3314	−1.3324	0.0254	0.0576	0.3033	−2.1630
3.2	0.3422	−1.0424	0.3309	−1.3241	0.0161	0.0384	0.3184	−2.3389
3.4	0.3430	−1.0456	0.3304	−1.3157	0.0106	0.0245	0.3291	−2.4571
3.6	0.3437	−1.0482	0.3301	−1.3091	0.0071	0.0155	0.3371	−2.5404
3.8	0.3443	−1.0506	0.3296	−1.3023	0.0047	0.0100	0.3431	−2.5995
4.0	0.3448	−1.0528	0.3293	−1.2974	0.0032	0.0066	0.3477	−2.6436

The remaining system is the anilide anion−HF complex (Chart 3; see Table 6). It can be seen that the ρ and $\nabla^2\rho$ values in the BCP of the C−N bond are less changeable than those in the previous case and increase slightly (as absolute values) when the complex becomes weaker. On the other hand, the N−H bond is strengthened for shorter N···F distances. This can be rationalized by assuming that the negative charge located partially on the N atom provides an antibonding orbital contribution to this bond. Therefore, when the hydrogen bridge is strengthened, the antibonding orbital of the N−H bond is depopulated, which results in an increase of the N−H BCP electron density. Indeed, the net atomic charge calculated for the nitrogen atom via both AIM and NBO methods is consistently negative for all of the complexes (see Table 7). Moreover, at a given N···F separation, it is most negative for the anilide anion−HF complex (e.g., at 3.0 Å, it is −1.045 for $PhNH_2$···HF, −1.127 for $PhNH_2$···F$^-$, and −1.184 for $PhNH^-$···HF). Summarizing the AIM study, it is worth mentioning that the charged complexes exhibit larger variability of the electron density and its Laplacian in BCPs, which is in

agreement with the SAPT analysis, emphasizing a significant role of polarization.

Natural Bond Orbitals. Application of the NBO approach allows one to look at mutual relations between the strength of the H-bond presented by the H···B intermolecular distance and the electron structure at all bonds linking the *ipso*-carbon atom (C1) with all neighboring atoms (C2, C6, and N; see Charts 1−3) and with the occupancy of orbitals at the nitrogen atom.

It results from scatter plots in Figure 7 that, for both cases where the nitrogen atom is a proton-accepting center ($PhNH^-\cdots HF$ and $PhNH_2\cdots HF$) the contribution of the p orbital in the C1−N bond increases with an increase of the H-bond strength, whereas in the case of NH_2 being the proton-donating group interacting with F^- ($PhNH_2\cdots F^-$), the dependence is opposite. To some extent, very similar regularity is observed for the contribution of the p orbital to bonds C1−C2 and C1−C6. In both former cases ($PhNH^-\cdots HF$ and $PhNH_2\cdots HF$), the percentage of the p orbital decreases with an increase of the H-bond strength, while in the latter ($Ph-NH_2\cdots F^-$), it increases. This is in line with the Bent−Walsh rule,[69,70] which states that if the substituent X in monosubstituted benzene derivatives is strongly electronegative, then the sp^2 orbital in the direction of CX contains more p character, that is, $sp^2 \rightarrow sp^{2+\delta}$. In both cases where nitrogen is a proton-accepting center, the electronegativity of the NH_2 or NH^- group increases,[45] and simultaneously along C1−C2 and C1−C6 bonds, the contribution of p decreases, $sp^2 \rightarrow sp^{2-\delta/2}$.

Some irregularities are observed when comparing the changes of the percentage of p in C1−C2 and C1−C6 for $PhNH^-\cdots HF$. A less steep dependence for the C1−C6 bond in this case may be explained by the effect similar to that known as the Angular Group Induced Bond Alternation (AGIBA),[71−73] which states that angular groups cause a nonsymmetrical bond length in the ring of monosubstituted species, that is, C1−C2 is different in length than C1−C6.

It results from Figure 8 that for all studied H-bonded systems, the occupancy of the σ orbital of the CN bond is practically independent of the strength of interaction, with a mean value of 1.992. Almost the same is a picture for the π orbital of the CN bond (empty diamonds and triangle in Figure 8), which exists for all $PhNH^-\cdots HF$ complexes, and in the case of a fully optimized $PhNH_2\cdots F^-$ complex, the occupancy is almost full. In the former case, its occupancy slightly increases with the strengthening of the interaction (from 1.977 up to 1.981) and reaches a maximal value (1.984) in the latter complex. Much more differentiated is a picture of occupancy of the orbital describing the lone pair (LP, color diamonds, triangles, and circles in Figure 8) at the nitrogen atom. In the case of charged $PhNH_2\cdots F^-$ and $PhNH^-\cdots HF$ complexes, the occupancy of the LP significantly decreases with an increase of the H-bond strength. For neutral $PhNH_2\cdots HF$ systems at the beginning, the occupancy of the LP slightly increases with the strengthening of the interaction (the N···F separation from 4.0 to 3.2 Å), then reaches a maximum, and then decreases similarly as in the former case. Moreover, in the latter complex as well as in the $PhNH^-\cdots HF$ one for the H-bond length, $d_{H\cdots B}$, ~1.7 Å, the occupancies of the lone pair are almost identical. The common feature of these complexes is the nitrogen atom acting as the proton acceptor. Note that the LP occupancy for the $PhNH^-\cdots HF$ complexes is always greater than that for the $PhNH_2\cdots F^-$ ones, which is related to the fact that in the first case the negative charge at the nitrogen atom for a particular N···F distance is more pronounced (see Table 7). The above-mentioned decrease of the nitrogen LP occupancy in all discussed cases seems to be associated with an involvement,

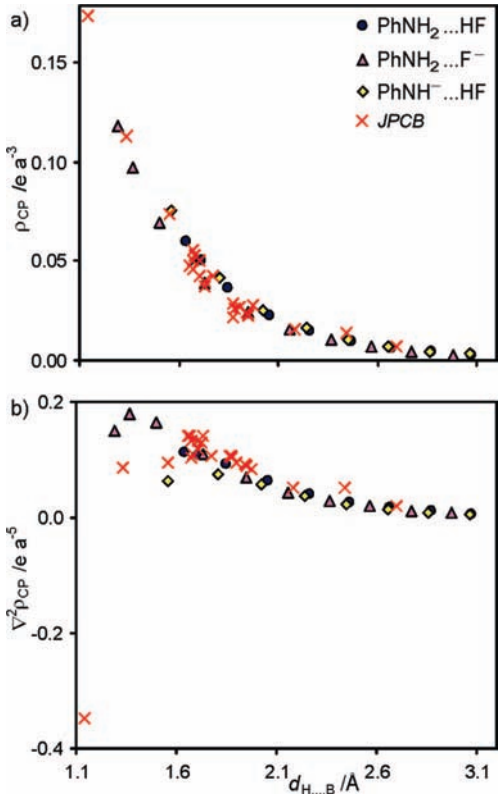

Figure 5. Dependence of electron density, ρ, and its Laplacian, $\nabla^2\rho$, on the length of the H-bond, $d_{H\cdots B}$, for complexes of aniline with HF and F^- and the anilide anion with HF. For comparison, data for a set of 25 equilibrium H-bonded complexes (ref 4) were added.

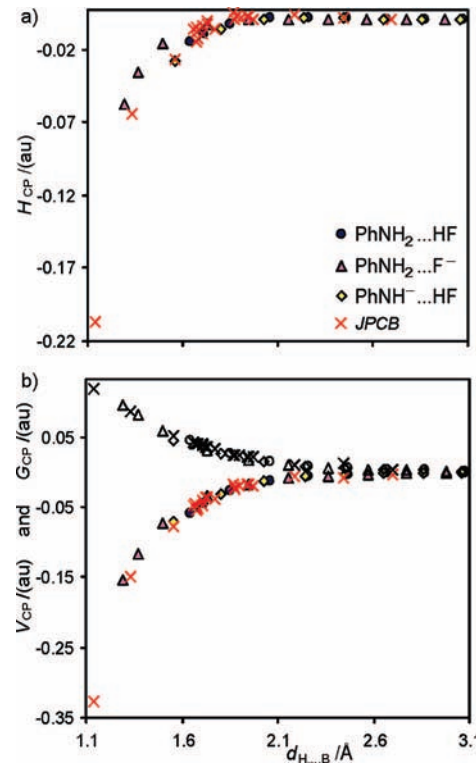

Figure 6. The total, H_{CP}, potential, V_{CP}, and kinetic, G_{CP}, electron energy density at the bond critical point of H-bonds versus the length of the H-bond, $d_{H\cdots B}$, for complexes of aniline with HF and F^- and the anilide anion with HF. For comparison, data for a set of 25 equilibrium H-bonded complexes (ref 4) were added.

TABLE 7: The NBO and AIM Net Atomic Charges on the Nitrogen Atom for the Three Studied Complexes As Functions of the N···F Separation

$PhNH_2$···HF			$PhNH_2$···F^-			$PhNH^-$···HF		
N···F distance /Å	NBO	AIM	N···F distance /Å	NBO	AIM	N···F distance /Å	NBO	AIM
			2.450[a]	−0.821	−1.178			
2.6	−0.832	−1.023	2.5	−0.817	−1.176			
2.671[a]	−0.836	−1.027	2.6	−0.813	−1.168	2.6	−0.911	−1.171
2.8	−0.840	−1.035	2.8	−0.813	−1.146	2.8	−0.933	−1.178
3.0	−0.839	−1.045	3.0	−0.812	−1.127	3.0	−0.940	−1.184
3.2	−0.835	−1.051	3.2	−0.809	−1.113	3.2	−0.940	−1.187
3.4	−0.829	−1.055	3.4	−0.805	−1.102	3.4	−0.935	−1.187
3.6	−0.824	−1.058	3.6	−0.802	−1.094	3.6	−0.929	−1.185
3.8	−0.819	−1.059	3.8	−0.799	−1.088	3.8	−0.923	−1.182
4.0	−0.815	−1.056	4.0	−0.798	−1.084	4.0	−0.917	−1.179

[a] N···F distance of the optimal B3LYP/6-311+G(d,p) structure.

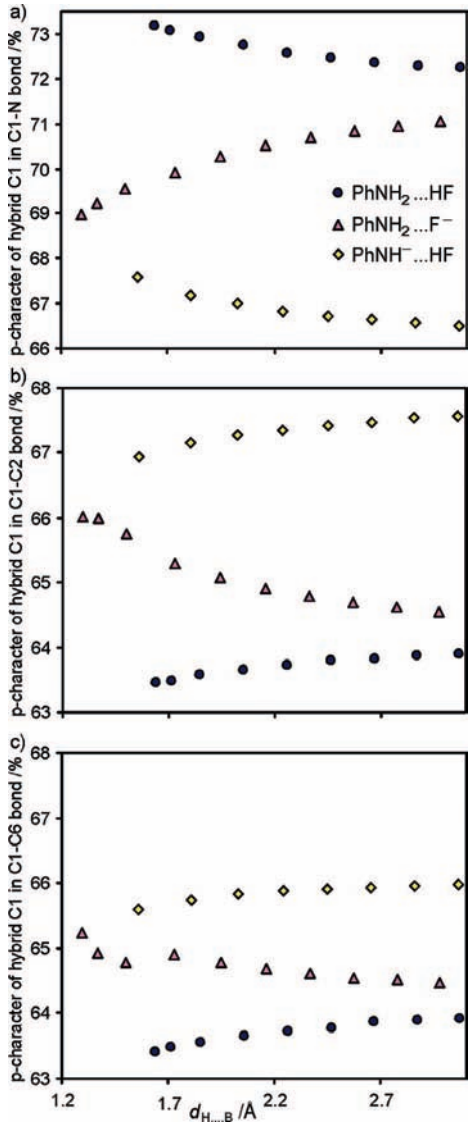

Figure 7. Effect of the H-bonding strength for $PhNH_2$···HF, $PhNH_2$···F^-, and $PhNH^-$···HF complexes on the percentage of the p character of sp^2 hybrids of the carbon atom C1 in its bonds (a) C1—N, (b) C1—C2, and (c) C1—C6 (see Charts 1−3).

directly or indirectly, of the electron pair in H-bond formation. This growing involvement at decreasing N···F distances is correlated with the systematic increase of the electron density Laplacian at the N···H critical point, reported by the AIM study (Tables 4 and 6).

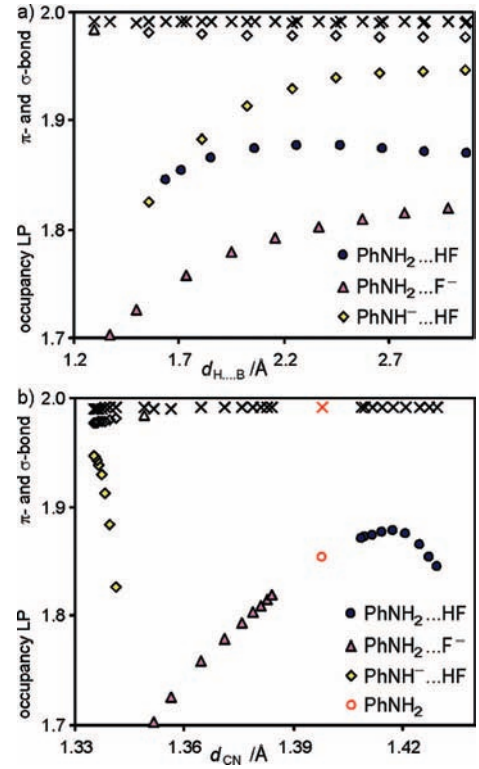

Figure 8. Dependence of the occupancies of the free sp^2/sp^3 orbital of the nitrogen, called the LP (color diamonds, triangles, and circles), the π contribution to the CN bond (empty diamonds and triangle), and the σ bond (crosses) on (a) the H-bond length, $d_{H\cdots B}$, and (b) the CN bond length, d_{CN}, for $PhNH_2$···HF, $PhNH_2$···F^-, and $PhNH^-$···HF complexes. The red signs mean noninteracting aniline.

IV. Conclusions

The H-bonded complexes of aniline with HF/F^- and anilide with HF, with the gradually changing strength of interaction, were used as model systems to study the interaction energy partitioning and electron density rearrangement in the middle strong neutral and charge-assisted hydrogen bonds. The results of all applied theories, SAPT, AIM, and NBO, clearly outline the differences between neutral ($PhNH_2$···HF) and anionic ($PhNH_2$···F^-, and $PhNH^-$···HF) complexes. The energies of interaction for neutral complexes are always less negative (a significantly weaker H-bond) than those for the charged ones, analogous with the strength of interaction in the H_2O···HOH and [HOH···OH]$^-$ systems.[63] The SAPT analysis showed the same picture for electrostatic and induction energy terms but not for the exchange and correction to the exchange resulting

from the polarization (exch−ind) ones, for which there is no distinction between those two forms of H-bonding. The electrostatic term is crucial for distinguishing between neutral and charge-assisted hydrogen bonds in the whole range of the simulated strength of interaction, whereas the induction one applies in the case of larger H···B distances. The most important change for anionic systems concerned the relationship between the electrostatic and exchange terms; while the first one grew significantly, the second one underwent only relatively small changes. The dispersion energy term does not seem to play a significant role in the total picture of the interaction energy for our model systems. The principal component analysis applied to independent terms obtained by SAPT energy decomposition showed that the first component describes 95% total variance, and the most important contributions to this component are electrostatic, induction, and exchange energies. Modeled H-bonded systems, $PhNH_2\cdots HF$, $PhNH_2\cdots F^-$, and $PhNH^-\cdots HF$, due to gradual changes in the N···F interatomic distance, are nonequilibrium ones and follow Popelier's criteria of the H-bond formation. Moreover, the electron density and its Laplacian at the bond critical point (BCP) of the hydrogen bond in these complexes behave in a similar way as those obtained for equilibrium systems, both as concerns experimental[38,39] and computational[4] data. According to the AIM parameters of selected bond critical points, the behavior of bonds in the vicinity of the H-bond is dependent on the type of complex (neutral versus anionic) and location of the negative charge. Larger variability of the electron density and its Laplacian in the BCP are exhibited by charged complexes, which is in agreement with the SAPT analysis, emphasizing a significant role of polarization. The Natural Bond Orbitals analysis showed that the LP occupancy for the $PhNH^-\cdots HF$ complexes is always greater than that for the $PhNH_2\cdots F^-$ ones. This is associated with the presence of a more negative charge (influx of electron density) at the nitrogen in the $PhNH^-\cdots HF$ complex (see Table 7). For all studied complexes, the occupancy of the lone pair at the nitrogen atom and the p character of sp^2 hybrids of the substituted carbon atom of the ring depend on the strength of the H-bond. Moreover, the changes of the percentage of the p character of all hybrid orbitals at this carbon atom follow the Bent−Walsh rule, in agreement with the experimental results.[46]

Acknowledgment. A.J. and J.J.P. gratefully acknowledge the Wrocław Center for Networking and Supercomputing (WCSS), the Academic Computer Center CYFRONET-KRAKÓW (Grants KBN/SGI/UWrocl/029/1998 and KBN/SGI/UWrocl/078/2001), and the Poznań Supercomputing and Networking Center for providing computer time and facilities. H.S. and T.M.K. thank the Interdisciplinary Center for Mathematical and Computational Modeling (Warsaw, Poland) for computational facilities, and H.S. thanks the Warsaw University of Technology for financial support.

References and Notes

(1) Categorizing Hydrogen Bonding and Other Intermolecular Interactions. IUPAC Project. www.iupac.org/projects/2004/2004−026−2-100.html.
(2) Galvez, O.; Gomez, P. C.; Pacios, L. F. *J. Chem. Phys.* **2001**, *115*, 11166–11184.
(3) Desiraju, G. R. *Acc. Chem. Res.* **2002**, *35*, 565–573.
(4) Grabowski, S. J.; Sokalski, W. A.; Dyguda, E.; Leszczynski, J. *J. Phys. Chem. B* **2006**, *110*, 6444–6446.
(5) Jeffrey, G. A. *An Introduction to Hydrogen Bonding*; Oxford University Press: Oxford, U.K., 1997; pp 12−16.
(6) Jeffrey, G. A.; Saenger, T. *Hydrogen Bonding in Biological Structures*; Springer: Berlin, Germany, 1991.
(7) Desiraju, G. R.; Steiner, T. *The Weak Hydrogen Bonding in Structural Chemistry and Biology*; Oxford University Press: Oxford, U.K., 1999.
(8) Meyer, E. A.; Castellano, R. K.; Diederich, F. *Angew. Chem., Int. Ed.* **2003**, *42*, 1210–1250.
(9) Biratha, K. *Cryst. Eng. Commun.* **2003**, *5*, 374–384.
(10) Nishio, M. *Cryst. Eng. Commun.* **2004**, *6*, 130–158.
(11) Kitagawa, S.; Uemura, K. *Chem. Soc. Rev.* **2005**, *34*, 109–119.
(12) Elstner, M.; Hobza, P.; Frauenheim, T.; Suhai, S.; Kaxiras, E. *J. Chem. Phys.* **2001**, *114*, 5149–5155.
(13) Branden, C.; Tooze, J. *Introduction to Protein Structure*, 2nd ed., Garland Publishing Inc.: New York, 1999.
(14) Wyttenbach, T.; Bowers, M. T. *Annu. Rev. Phys. Chem.* **2007**, *58*, 511–533.
(15) Fairall, C. W.; Reese, W. *Phys. Rev. B* **1975**, *11*, 2066–2068.
(16) Jeffrey, G. A. *An Introduction to Hydrogen Bonding*; Oxford University Press: Oxford, U.K., 1997; pp 113−116.
(17) Gilli, G.; Bellucci, F.; Ferretti, V.; Bertolasi, V. *J. Am. Chem. Soc.* **1989**, *111*, 1023–1028.
(18) Gilli, P.; Bertolasi, V.; Ferretti, V.; Gilli, G. *J. Am. Chem. Soc.* **1993**, *116*, 909–915.
(19) Gilli, G.; Gilli, P. *J. Mol. Struct.* **2000**, *522*, 1–15.
(20) Ward, M. D. *Chem. Commun.* **2005**, 5838–5842.
(21) Sobczyk, L.; Grabowski, S. J.; Krygowski, T. M. *Chem. Rev.* **2005**, *105*, 3513–3560.
(22) Cleland, W. W.; Frey, P. A.; Gerlt, J. A. *J. Biol. Chem.* **1998**, *273*, 25529–25532.
(23) Scheiner, S. *Hydrogen Bonding. A Theoretical Perspective*; Oxford University Press: Oxford, U.K., 1997.
(24) Kitaura, K.; Morokuma, K. *Int. J. Quantum Chem.* **1976**, *10*, 325–340.
(25) Sokalski, W. A.; Roszak, S.; Pecul, K. *Chem. Phys. Lett.* **1988**, *153*, 153–159.
(26) Mo, Y.; Peyerimhoff, S. D. *J. Chem. Phys.* **1998**, *109*, 1687–1697.
(27) Mo, Y. *J. Chem. Phys.* **2003**, *119*, 1300–1306.
(28) Mo, Y.; Song, L.; Wu, W.; Cao, Z.; Zhang, Q. *J. Theor. Comput. Chem.* **2002**, *1*, 137–151.
(29) Kawamura, Y.; Nakai, H. *J. Comput. Chem.* **2004**, *25*, 1882–1887.
(30) Ababou, A.; van der Waart, A.; Gogonea, V.; Merz, K. M., Jr. *Biophys. Chem.* **2007**, *125*, 221–236.
(31) Jeziorski, B.; Moszyñski, R.; Szalewicz, K. *Chem. Rev.* **1994**, *94*, 1887–1930.
(32) Bader, R. F. W. *Atoms in Molecules, A Quantum Theory*; Clarendon Press: Oxford, U.K., 1990.
(33) Bader, R. F. W.; Beddall, P. M. *J. Chem. Phys.* **1972**, *56*, 3320–3329.
(34) Koch, U.; Popelier, P. L. A. *J. Phys. Chem.* **1995**, *99*, 9747–9754.
(35) Platts, J. A. *Phys. Chem. Chem. Phys.* **2000**, *2*, 973–980.
(36) Platts, J. A. *Phys. Chem. Chem. Phys.* **2000**, *2*, 3115–3120.
(37) Hocquet, A. *Phys. Chem. Chem. Phys.* **2001**, *3*, 3192–3199.
(38) Malinson, P. R.; Smith, G. T.; Wilson, C. C.; Grech, E.; Wozniak, K. *J. Am. Chem. Soc.* **2003**, *125*, 4259–4270.
(39) Dominiak, P. M.; Makal, A.; Mallinson, P. R.; Trzcinska, K.; Eilmes, J.; Grech, E.; Chruszcz, M.; Minor, W.; Wozniak, K. *Chem.−Eur. J.* **2006**, *12*, 1941–1949.
(40) Panek, J. J.; Jezierska, A.; Mierzwicki, K.; Latajka, Z.; Koll, A. *J. Chem. Inf. Model.* **2005**, *45*, 39–48.
(41) Panek, J. J.; Jezierska, A.; Vračko, M. *J. Chem. Inf. Model.* **2005**, *45*, 264–272.
(42) Parthasarathi, R.; Sundar Raman, S.; Subramanian, V.; Ramasami, T. *J. Phys. Chem. A* **2007**, *111*, 7141–7148.
(43) Weinhold, F.; Landis, C. R. *Valency and Bonding. A Natural Bond Orbital Donor−Acceptor Perspective*; Cambridge University Press; Cambridge, U.K., 2005.
(44) Szatyłowicz, H.; Krygowski, T. M.; Hobza, P. *J. Phys. Chem. A* **2007**, *111*, 170–175.
(45) Szatyłowicz, H.; Krygowski, T. M. *J. Mol. Struct.* **2007**, *844−845*, 200–207.
(46) Szatyłowicz, H.; Krygowski, T. M.; Zachara-Horeglad, J. E. *J. Chem. Inf. Model.* **2007**, *47*, 875–886.
(47) Cheng, M.; Pu, X.; Wong, N.-B.; Li, M.; Tian, A. *New J. Chem.* **2008**, *32*, 1060–1070.
(48) Hohenberg, P.; Kohn, W. *Phys. Rev.* **1964**, *136*, B864–B871.
(49) Kohn, W.; Sham, L. J. *Phys. Rev.* **1965**, *140*, A1133–A1138.
(50) Becke, A. D. *J. Chem. Phys.* **1993**, *98*, 5648–5652.
(51) Lee, C.; Yang, W.; Parr, R. G. *Phys. Rev. B* **1988**, *37*, 785–789.
(52) Krishnan, R.; Binkley, J. S.; Seeger, R.; Pople, J. A. *J. Chem. Phys.* **1980**, *72*, 650–654.
(53) Frisch, M. J. Trucks, G. W.; Schlegel, H. B.; Scuseria, G. E.; Robb, M. A.; Cheeseman, J. R.; Montgomery, J. A., Jr.; Vreven, T.; Kudin, K. N.; Burant, J. C.; Millam, J. M.; Iyengar, S. S.; Tomasi, J.; Barone, V.; Mennucci, B.; Cossi, M.; Scalmani, G.; Rega, N.; Petersson, G. A.; Nakatsuji, H.; Hada, M.; Ehara, M.; Toyota, K.; Fukuda, R.; Hasegawa, J.; Ishida, M.; Nakajima, T.; Honda, Y.; Kitao, O.; Nakai, H.; Klene, M.; Li, X.; Knox, J. E.; Hratchian, H. P.; Cross, J. B.; Bakken, V.; Adamo, C.; Jaramillo, J.; Gomperts, R.; Stratmann, R. E.; Yazyev, O.; Austin, A. J.;

Cammi, R.; Pomelli, C.; Ochterski, J. W.; Ayala, P. Y.; Morokuma, K.; Voth, G. A.; Salvador, P.; Dannenberg, J. J.; Zakrzewski, V. G.; Dapprich, S.; Daniels, A. D.; Strain, M. C.; Farkas, O.; Malick, D. K.; Rabuck, A. D.; Raghavachari, K.; Foresman, J. B.; Ortiz, J. V.; Cui, Q.; Baboul, A. G.; Clifford, S.; Cioslowski, J.; Stefanov, B. B.; Liu, G.; Liashenko, A.; Piskorz, P.; Komaromi, I.; Martin, R. L.; Fox, D. J.; Keith, T.; Al-Laham, M. A.; Peng, C. Y.; Nanayakkara, A.; Challacombe, M.; Gill, P. M. W.; Johnson, B.; Chen, W.; Wong, M. W.; Gonzalez, C.; Pople, J. A. *Gaussian 03*, revision A.1; Gaussian, Inc.: Pittsburgh, PA, 2003.

(54) Schmidt, M. W.; Baldridge, K. K.; Boatz, J. A.; Elbert, S. T.; Gordon, M. S.; Jensen, J. H.; Koseki, S.; Matsunaga, N.; Nguyen, K. A.; Su, S. J.; Windus, T. L.; Dupuis, M.; Montgomery, J. A. *J. Comput. Chem.* **1993**, *14*, 1347–1363.

(55) (a) Williams, H. L.; Szalewicz, K.; Jeziorski, B.; Moszynski, R.; Rybak, S. *J. Chem. Phys.* **1993**, *98*, 1279–1292. (b) Bukowski, R.; Sadlej, J.; Jeziorski, B.; Jankowski, P.; Szalewicz, K.; Kucharski, S. A.; Williams, H. L.; Rice, B. M. *J. Chem. Phys.* **1999**, *110*, 3785–3803.

(56) (a) Milet, A.; Moszynski, R.; Wormer, P. E. S.; van der Avoird, A. *J. Phys. Chem. A* **1999**, *103*, 6811–6819. (b) Cybulski, H.; Sadlej, J. *J. Chem. Theory Comput.* **2008**, *4*, 892–897.

(57) Bukowski, R.; Cencek, W.; Jankowski, P.; Jeziorski, B.; Jeziorska, M.; Kucharski, S. A.; Lotrich, V. F.; Misquitta, A. J.; Moszyński, R.; Patkowski, K.; Podeszwa, R.; Rybak, S.; Szalewicz, K.; Williams, H. L.; Wheatley, R. J.; Wormer, P. E. S. and Żuchowski, P. S. *SAPT2006: An Ab Initio Program for Many-Body Symmetry-Adapted Perturbation Theory Calculations of Intermolecular Interaction Energies*; see http://www.physics.udel.edu/∼szalewic/SAPT/SAPT.html.

(58) Popelier, P. L. A. *Atoms in Molecules—An Introduction*; Pearson Education; Harlow,U.K., 2000.

(59) Bader, R. F. W. *AIMPAC, Suite of Programs for the Theory of Atoms in Molecules*; McMaster University, Hamilton, Ontario, Canada, 1991.

(60) (a) Foster, J. P.; Weinhold, F. *J. Am. Chem. Soc.* **1980**, *102*, 7211–7218. (b) Reed, A. E.; Weinhold, F. *J. Phys. Chem.* **1983**, *78*, 4066–4073. (c) Reed, A. E.; Weinstock, R. B.; Weinhold, F. *J. Phys. Chem.* **1985**, *83*, 735–746. (d) Reed, A. E.; Weinhold, F. *J. Phys. Chem.* **1985**, *83*, 1736–1740. (e) Carpenter, J. E.; Weinhold, F. *J. Mol. Struct.: THEOCHEM* **1988**, *169*, 41–62. (f) Reed, A. E.; Curtis, L. A.; Weinhold, F. *Chem. Rev.* **1988**, *88*, 899–926.

(61) Humphrey, W.; Dalke, A.; Schulten, K. *J. Mol. Graph.* **1996**, *14*, 33–38.

(62) Boys, S. F.; Bernardi, F. *Mol. Phys.* **1970**, *19*, 553–556.

(63) Remer, L. C.; Jensen, J. H. *J. Phys. Chem. A* **2000**, *104*, 9266–9275.

(64) Bandyopadhyay, I.; Lee, H. M.; Kim, K. S. *J. Phys. Chem. A* **2005**, *109*, 1720–1728.

(65) Panek, J. J.; Jezierska, A. *J. Phys. Chem. A* **2007**, *111*, 650–655.

(66) Zalewski, R. I. In *Similarity Models in Organic Chemistry, Biochemistry and Related Fields*; Zalewski, R. I.; Krygowski, T. M.; Shorter, J., Eds.; Elsevier: Amsterdam, The Netherlands, 1991; Chapter 9, pp 455−556.

(67) (a) Pacios, L. F.; Gálvez, O.; Gómez, P. C. *J. Chem. Phys.* **2005**, *122*, 1–11. (b) Pacios, L. F. In *Hydrogen Bonding—New Insights*, (Challenges and Advances in Computational Chemistry and Physics, 3); Grabowski, S. J., Ed.; Springer: Dordrecht, The Netherlands, 2006; pp 109−148.

(68) (a) Espinosa, E.; Lecomte, C.; Ghermani, N. E.; Devemy, J.; Rohmer, M. M.; Benard, M.; Molins, E. *J. Am. Chem. Soc.* **1996**, *118*, 2501–2502. (b) Espinosa, E.; Molins, E.; Lecomte, C. *Chem. Phys. Lett.* **1998**, *285*, 170–173. (c) Espinosa, E.; Molins, E. *J. Chem. Phys.* **2000**, *113*, 5686–5694. (d) Espinosa, E.; Alkorta, I.; Elguero, J.; Molins, E. *J. Chem. Phys.* **2002**, *117*, 5529–5542. (e) Espinosa, E.; Alkorta, I.; Mata, I.; Molins, E. *J. Phys. Chem. A* **2005**, *109*, 6532–6539. (f) Mata, I.; Molins, E.; Alkorta, I.; Espinosa, E. *J. Phys. Chem. A* **2007**, *111*, 6425–6433.

(69) (a) Walsh, A. D. *Discuss. Faraday Soc.* **1947**, *2*, 18–25. (b) Bent, H. A. *Chem. Rev.* **1961**, *61*, 275–311.

(70) Domenicano, A.; Vaciago, A.; Coulson, C. A. *Acta Crystallogr., Sect. B* **1975**, *31*, 1630–1641.

(71) Krygowski, T. M.; Anulewicz, R.; Jarmula, A.; Bak, T.; Rasala, D.; Howard, S. *Tetrahedron* **1994**, *50*, 13155–13164.

(72) Krygowski, T. M.; Anulewicz, R.; Hiberty, P. C. *J. Org. Chem.* **1996**, *61*, 8533–8535.

(73) Krygowski, T. M.; Wisiorowski, M.; Howard, S. T.; Stolarczyk, L. Z. *Tetrahedron* **1997**, *53*, 13027–13036.

JP803592V